This full text paper was peer reviewed at the direction of IEEE Communications Society subject matter experts for publication in the IEEE INFOCOM 2009 proceedings.

Medium access control for 60 GHz outdoor mesh networks with highly directional links

R. Mudumbai, S. Singh and U. Madhow
Dept. of Electrical and Computer Engineering
University of California, Santa Barbara, CA 93106
Email:[raghu,sumit,madhow]@ece.ucsb.edu

***Abstract*—We investigate an architecture for multi-Gigabit outdoor mesh networks operating in the unlicensed 60 GHz "millimeter (mm) wave" band. In this band, the use of narrow beams is essential for attaining the required link ranges in order to overcome the higher path loss at mm wave carrier frequencies. However, highly directional links make standard MAC methods for interference management, such as carrier sense multiple access, which rely on neighboring nodes hearing each other, become inapplicable. In this paper, we study the extent to which we can reduce, or even dispense with, interference management, by exploiting the reduction in interference due to the narrow beamwidths and the oxygen absorption characteristic of the 60 GHz band. We provide a probabilistic analysis of the interference incurred due to uncoordinated transmissions, and show that, for the parameters considered, the links in the network can be thought of as *pseudo-wired.* That is, interference can essentially be ignored in MAC design, and the challenge is to schedule half-duplex transmissions in the face of the "deafness" resulting from highly directional links. We provide preliminary simulation results to validate our approach.**

I. Introduction

Recent progress in RFIC design in the mm-wave band has spurred significant recent interest in 60 GHz networks for indoor multimedia applications, including standardization efforts within the IEEE 802.15.3c (WPAN) and 802.11 (WLAN) task groups. However, use of the 60 GHz band is also very attractive for *outdoor* mesh networks with multiGigabit links at relatively short ranges (of the order of 100 meters). Such mm wave mesh networks can serve as a high-speed backhaul needed for broadband connectivity where there is limited wired or optical infrastructure. In this paper, we take the first steps towards defining an architecture for such outdoor mm wave networks, accounting for the unique characteristics of mm wave communication.

The fundamental distinguishing feature of the 60 GHz band relative to, say, the 2.4 GHz WiFi band, is the order of magnitude difference in wavelength. The free space propagation loss of electromagnetic waves scales as λ^2, and (fixing the antenna apertures at each end), the directivity scales as $\frac{1}{\lambda^2}$ where λ is the carrier wavelength. Thus, the overall path-loss varies as $\frac{1}{\lambda^2}$; this corresponds to a net *gain* of 28 dB in going from 2.4 GHz to 60 GHz. This is fortunate: given the RF power constraints of low-cost silicon implementations, employing highly directive antennas at both transmitter and receiver is *essential* for the range/rate combinations we wish to achieve. The small wavelength in the mm-wave band allows the design of nodes with a compact form factor (comparable to a WiFi access point) that can achieve directivities of around 25 dBi quite easily.

The use of electronic beamsteering with highly directional links opens up a number of questions in network design, and we focus on the most fundamental of these in this paper: medium access control (MAC). If neighbors can no longer hear each other, protocols such as CSMA/CA, or variants thereof designed for the mildly directional links possible at lower carrier frequencies, simply do not work. At the same time, the highly directional transmissions lead to vastly reduced interference between nearby transmissions, which raises the interesting possibility that high level of interference management provided by conventional MAC protocols may not be needed for networks in the mm-wave band. In this paper, we use a statistical analysis of interference to show that, for the antenna directivities of interest to us, even uncoordinated transmission for different transmit-receive pairs leads to small collision probabilities. This motivates a *pseudo-wired* abstraction to serve as a first order approximation of mm-wave wireless links, and provide insights to guide MAC design. Under this abstraction, transmissions on different links do not interfere with each other. However, unlike a truly wired node, mm-wave network nodes have a half-duplex constraint, i.e. they can only send or receive at a given time. This allows MAC designers to concentrate on developing lightweight protocols whose purpose is to schedule in a "deaf" network, subject to half-duplex constraints.

Related Work. Directional networking for cellular, broadband, and WiFi-based multihop wireless networks operating over lower frequency bands has been extensively studied in previous work [1]–[3]. In [4], [5], it was shown that directional transmission improves the connectivity of ad-hoc networks by establishing long-range links even without using smart beamsteering (i.e. using randomly directed beams). Most of the directional networking proposals for multihop wireless networks employ a separate omni-directional mode for protocol operation in order to avoid the coordination issues that arise

This work was supported by the National Science Foundation under grants CNS-0520335, ECS-0636621 and CNS-0832154, by the Office for Naval Research under grant N00014-06-1-0066, and by the Institute for Collaborative Biotechnologies under grant DAAD19-03-D-0004 from the US Army Research Office.

from being fully directional (such as neighbor discovery and deafness). This dual-mode operation is not appropriate for the mm wave mesh networks, where very high directionality is required simply to achieve a reliable high data rate link. Furthermore, the directivity achievable at the lower frequency bands is much smaller, so that the focus of MAC design in previous work on directional networking is still on interference management. To the best of our knowledge, the present paper is the first to consider mm wave mesh networks, and show quantitatively that the very high antenna directivities lead to very low levels of interference even with uncoordinated transmissions.

II. Network Model

For our interference analysis, we consider a Poisson distribution of nodes over a large area with a density ρ_s. If we now randomly select a subset of N_T nodes as transmitters, the distribution of transmitters on the area of interest is also Poisson, with density $\rho = \rho_s p_t$ where p_t is the probability that the selected node is transmitting. For a large deployment area A, we have $\rho \approx \frac{N_T}{A}$.

We assume that all the nodes have already completed a network discovery procedure, and thus know how to steer their antennas to each of their neighbors. We also assume that each node can communicate with at most one other node at any given time slot. In other words, we do not rely on advanced physical layer capabilities such as spatial multiplexing or multi-user detection. If multiple neighbors are transmitting to the same receiver, at most one of them can be successfully decoded by the receiver. All other transmissions in the network act as interference for the receiver. The amount of interference depends on the location of the interferer relative to the receiver, and the radiation patterns of the antennas at the receiver and the interferer. We assume that a transmission is successfully decoded by the receiver if the total signal to interference and noise ratio (SINR) is above a given threshold, say $\beta = 15$ dB (which allows for uncoded QPSK modulation at a BER of $< 10^{-9}$). Otherwise, a *collision* occurs and the transmission is lost.

The standard Friis transmission equation gives the received power as a function of range r as

$$P_R(r) = P_T G_R G_T \Big(\frac{\lambda}{4\pi r}\Big)^2 e^{-\alpha r} \tag{1}$$

where P_T is the transmitted power, G_R, G_T are the gains of the receive and transmit antennas respectively, λ is the wavelength, and α is the attenuation factor due to absorption in the medium. For a mm wave link at 60 GHz, $\lambda = 5$ mm and α can be as high as 15 dB/km. Since lower absorption rates leads to *more* interference, we use the conservative value of $\alpha = 10$ dB/km in our numerical results.

Consider the link budget for a 2 Gbps Line of Sight (LoS) link at a range of $R_0 = 100$m, which provides a baseline for the rest of the paper. Assuming QPSK signaling, a desired SNR of 15 dB, oxygen absorption loss of 10 dB/km, and 10 mW transmit power, we need antenna gains of about 24 dBi at both transmitter and receiver in order to provide a 10 dB link margin.

A. Directional Antenna Model

Directional antennas are characterized by their pattern functions that measure the power gain $G(\phi, \theta)$ over the spherical azimuthal and elevation angle coordinates ϕ, θ. We assume that all nodes are on the same horizontal plane, and do not consider variation in beam pattern over the elevation angle θ, and work with the normalized 2-dimensional pattern

$$g(\phi) \triangleq \frac{G(\phi, 0)}{G_{max}} \text{ where } G_{max} = \max_{\phi} G(\phi, 0) \tag{2}$$

The azimuthal beamwidth of the antenna is then given by

$$\Delta\phi = \int_{\phi=-\pi}^{\pi} g(\phi) d\phi \tag{3}$$

One idealization that proves to be very useful for our interference analysis is that of a sectorized "flat-top" directional antenna, which has unit gain within its beamwidth and zero gain outside. More precisely,

$$g(\phi) = \begin{cases} 1, & |\phi| \le \frac{\Delta\phi}{2}, \\ 0, & \text{otherwise} \end{cases} \tag{4}$$

While the flat-top antenna is an useful idealization, practical directional antenna gains have a more complex dependence on the azimuth angle. For instance, sidelobes in the gain function could cause significant interference even in directions far from the antenna boresight. While exact computation of the gain functions of practical mm-wave antenna arrays can be messy (because array elements usually are directional themselves), we can obtain useful models with some simplifying assumptions. In particular, we obtain the following gain function for an N element linear array in which each individual flat-top element has beamwidth $\Delta\phi_0$:

$$g(\phi) = \begin{cases} \frac{1}{N} \frac{\sin(\frac{N}{2}\pi \sin\phi)}{\sin(\frac{1}{2}\pi \sin\phi)}, & |\phi| \le \frac{\Delta\phi_0}{2}, \\ 0, & \text{otherwise} \end{cases} \tag{5}$$

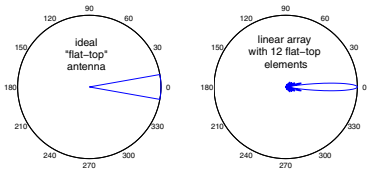

Fig. 1. Gain pattern for a flat-top antenna and a linear array of flat-top elements.

Fig. 1 shows the beam patterns for a narrow beam flat-top antenna and a 12-element linear array of broad-beam flat-top elements. The beamwidth in both cases (as defined as in (3)) is the same, 20°.

III. Interference Analysis

We now investigate the validity of a pseudo-wired model for the links in a mm wave mesh network, by analyzing the probability of packet failure for uncoordinated transmissions. Consider the transmitter-receiver pair shown in Fig. 2; without

loss of generality, assume that the receiver is located at the origin and is communicating with the transmitter located along the X-axis, at a distance less than or equal to the reference link distance R_0 while undergoing interference from other concurrent transmissions. The other $N_T - 1$ interfering transmitters are randomly placed over the area A, and are transmitting to receivers located at randomly chosen orientations.

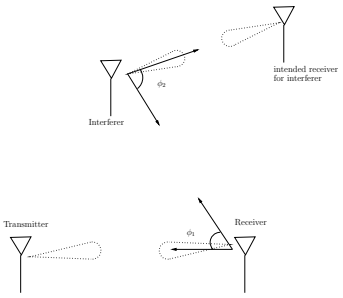

Fig. 2. The geometry of interference with directional antennas.

In their well-known work on wireless network capacity [6], Gupta et al introduce two different models of interference. In the *protocol model*, a packet loss occurs if and only if there is some interfering node whose signal at the receiver exceeds a given threshold. In the *physical model*, a packet loss occurs when the *total* interference from all nodes exceeds a given threshold. The models are summarized as follows:

$$\Pr(\text{collision}) \triangleq \begin{cases} \Pr\left(\max_k P_k \geq \frac{1}{\beta} P_0\right), & \text{(protocol model)} \\ \Pr\left(\sum_{k=1}^{N_T-1} P_k \geq \frac{1}{\beta} P_0\right), & \text{(physical model)} \end{cases}$$

where P_k is the power at the receiver of the signal from the k'th interferer. Since $\sum_k P_k \geq \max_k P_k$, it follows that the $\Pr(\text{collision})$ for the physical model is lower-bounded by the corresponding value for the protocol model. We first derive an expression for the collision probability under the protocol model for the flat-top antenna, and extend the derivation to more general directional antennas, and then to the physical model. Our derivation is similar to the analysis of localization error in [7].

A. Protocol model with ideal flat-top antennas

For the ideal flat-top antenna, only interferers located within the boresight of the receiver can cause a collision. Further, a transmitting node within this sector causes interference only if the receiver is within its boresight, which has probability $q = \frac{\Delta\phi}{2\pi}$ (since the potentially interfering transmitter is sending to a randomly chosen receiver). Let R_i be the *interference range* i.e. the maximum distance an interferer can be from the receiver and still cause a collision. Using (1), the signal and interference powers are evaluated as:

$$P_R \equiv P_0 = P_T G_{max}^2 \Big(\frac{\lambda}{4\pi R_0}\Big)^2 e^{-\alpha R_0} \tag{6}$$

$$P_{interf} = P_T G_{max}^2 \Big(\frac{\lambda}{4\pi R_i}\Big)^2 e^{-\alpha R_i} \tag{7}$$

where we used $G_T = G_R = G_{max}$ for the antenna gains assuming that the interferer and the receiver are within each other's boresights. We set $P_R = P_0$: when the transmitter and receiver are steered towards each other, this is the signal power designed for at the reference distance R_0. Using the collision condition $P_{interf} \geq \frac{1}{\beta} P_0$, we can rewrite (7) as:

$$\frac{R_i^2}{R_0^2} e^{\alpha(R_i - R_0)} = \beta \tag{8}$$

which determines R_i as a function of the SINR threshold β.

The number of potentially interfering transmitters is therefore a Poisson random variable with mean ρA_i, where $A_i = \frac{1}{2}\Delta\phi R_i^2$. The probability of any of these actually causing a collision is q, so that the number of interferers N_i causing a collision is also Poisson, with mean $q\mu_i$. The probability of a collision is therefore given by

$$\begin{aligned} \Pr(\text{collision}) &\equiv \Pr(N_i > 0) = 1 - e^{-q\mu_i} \qquad (9) \\ &= 1 - e^{-\frac{(\Delta\phi)^2}{4\pi}\rho R_i^2} \equiv 1 - e^{-\beta\rho R_0^2 A_c}, \\ \text{where } A_c &\triangleq \frac{(\Delta\phi)^2}{4\pi} e^{-\alpha(R_i - R_0)} \qquad (10) \end{aligned}$$

For a beamwidth of $\Delta\phi = 10^\circ$, $\beta = 15$ dB and $\rho R_0^2 = 1$ (corresponding to roughly $\pi\rho R_0^2 \approx 3$ transmitting nodes within communication range of each receiver), (10) gives an estimate of $\Pr(\text{collision}) \approx 3.7\%$, which suggests that acceptable MAC performance may be possible with minimal coordination for interference management.

B. Protocol model with general directional antennas

We now generalize (10) to a general directional antenna. We first compute the probability of collision due to a single interferer at a fixed location at a distance r, and angle ϕ_1 relative to the receiver as shown in Fig. 2. The angle ϕ_2 represents the direction of the interferer's beam relative to the receiver. We model ϕ_1, ϕ_2 as independent and uniformly distributed over $(-\pi, \pi]$, given the random orientation of the interfering transmitter and its beam relative to the desired receiver. Signal power is still given by (6), and the interference power is:

$$P_{interf} = P_T G_{max}^2 g(\phi_1) g(\phi_2) \Big(\frac{\lambda}{4\pi r}\Big)^2 e^{-\alpha r} \tag{11}$$

where we used $G_R = G_{max} g(\phi_1)$ and $G_T = G_{max} g(\phi_2)$. Using (6), we can rewrite (11) as

$$P_{interf} = P_0 g(\phi_1) g(\phi_2) \Big(\frac{R_0}{r}\Big)^2 e^{-\alpha(r - R_0)} \tag{12}$$

Therefore the probability $p_c(r, \phi_1)$ that this interferer would cause a collision is

$$\begin{aligned} p_c(r, \phi_1) &\triangleq \Pr\left(P_{interf} \geq \frac{1}{\beta} P_0\right) \\ &= \Pr\left(g(\phi_1) g(\phi_2) \geq \frac{1}{\beta} \big(\frac{r}{R_0}\big)^2 e^{\alpha(r - R_0)}\right) \\ &= \frac{1}{2\pi} \int_{-\pi}^{\pi} 1\Big(g(\phi_1) g(\phi_2) \geq \frac{1}{\beta} \big(\frac{r}{R_0}\big)^2 e^{\alpha(r - R_0)}\Big) d\phi_2 \qquad (13) \end{aligned}$$

where $1(.)$ is the indicator function that takes the value 1 when its argument is true, and 0 otherwise.

Consider now an interferer placed at random within a large area A. Then the probability of collision $\hat{p}_c$ can be obtained by averaging (13) over all possible positions of the interferer:

$$\begin{aligned}\hat{p}_c &= \frac{1}{A}\int\int_{(r,\phi_1)\in A} p_c(r,\phi_1)\ r dr\ d\phi_1 \\ &= \frac{\beta R_0^2}{A}\int\int_{\hat{r},\phi_1} p_c\big(\sqrt{\beta}R_0\hat{r},\phi_1\big)\ \hat{r}d\hat{r}\ d\phi_1 \end{aligned} \quad (14)$$

where we set $\hat{r} \triangleq \frac{1}{\sqrt{\beta}}\frac{r}{R_0}$, i.e. $\hat{r}$ is the distance of the interferer normalized to the reference link distance R_0 and interference threshold β. Using (13) in (14), we get

$$\hat{p}_c = \frac{\beta R_0^2}{2\pi A}\int\int_{\hat{r},\phi_1}\int_{\phi_2=-\pi}^{\pi} 1\Big(g(\phi_1)g(\phi_2) \geq \hat{r}^2 e^{\alpha R_0\left(\sqrt{\beta}\hat{r}-1\right)}\Big) \; d\phi_2\ \hat{r}d\hat{r}\ d\phi_1 \quad (15)$$

We now let the area A become infinitely large and cover the whole plane. From (2), $g(\phi_1)$ and $g(\phi_2)$ are upper-bounded by 1. We therefore only need to consider $\hat{r} \leq e^{\frac{\alpha R_0}{2}}$ in (15), because the argument of the indicator function $1(.)$ in (15) is always false outside this range. Then we have

$$\hat{p}_c = \beta R_0^2 \frac{A_c}{A}, \text{ where} \quad (16)$$

$$A_c \triangleq \frac{1}{2\pi}\int_{\hat{r}=0}^{e^{\frac{\alpha R_0}{2}}}\int_{\phi_1,\phi_2=-\pi}^{\pi} 1\Big(g(\phi_1)g(\phi_2) \geq \hat{r}^2 e^{\alpha R_0\left(\sqrt{\beta}\hat{r}-1\right)}\Big) \; d\phi_2\ \hat{r}d\hat{r}\ d\phi_1 \quad (17)$$

We now consider $N_T - 1 = \rho A$ interferers placed randomly in the area A. Each interferer has a collision probability $\hat{p}_c$ with the receiver given by (16). A collision occurs if at least one of these interferers cause a collision, and its probability is given by

$$\begin{aligned}\Pr(\text{collision}) &= 1-(1-\hat{p}_c)^{N_T-1} = 1-\lim_{A\to\infty}\big(1-\beta R_0^2\frac{A_c}{A}\big)^{\rho A} \\ &= 1-e^{-\beta\rho R_0^2 A_c} \end{aligned} \quad (18)$$

Since (18) has an identical form to (10), the collision probability depends on the antenna pattern only through A_c. Thus, for the protocol model, we can restrict attention to an equivalent flat-top model whose beamwidth can be calculated from (10) and (16) as $\Delta\phi_{eq} \triangleq \sqrt{4\pi A_c}e^{\frac{\alpha}{2}(R_i-R_0)}$. For instance, a linear 24-element linear array of flat-top antennas of sector size 120° and half-wavelength spacing has an equivalent "flat-top" beamwidth of about 15° for $\alpha = 10$ dB/km. Fig. 3 shows the equivalent "flat-top" beamwidths for linear arrays of different numbers of flat-top elements and half-wavelength spacing; as seen from the figure, the "flat-top" beamwidth is numerically close to the algebraic beamwidth given by (3) and does not vary much with the SINR threshold β.

C. Physical Model

In the protocol model, only nodes located within a bounded distance from the receiver are capable of causing a collision. On the other hand, for the physical model, interfering signals from a large number of far-away transmitters could, in principle, sum up at a desired receiver to cause packet failure. It turns out that traditional upper bound techniques such as Chernoff and Markov-type bounds do not work well when characterizing sum interference over a large area. We therefore use a hybrid approach, using an analytical Markov upper bound to characterize the effect of "far-away" interferers, and characterizing the sum interference from interferers within a bounded region through Monte-Carlo simulations. Let r_k be the distance of the k'th interferer from the receiver. We write the total interference power as the sum of two contributions P_{near} and P_{far}, defined as:

$$P_{near} \triangleq \sum_{\{k:r_k\leq R_{th}\}} P_k, \text{ and } P_{far} \triangleq \sum_{\{k:r_k>R_{th}\}} P_k \quad (19)$$

where R_{th} is a suitable large distance, say $R_{th} = 40R_0$. Then we have

$$\begin{aligned}&\Pr(\text{collision}) = \Pr\left(P_{near}+P_{far} \geq \frac{1}{\beta}P_0\right) \\ &\leq \Pr\left(P_{far} \geq \frac{1}{\beta}\Delta P\right) + \Pr\left(P_{near} \geq \frac{1}{\beta}(P_0-\Delta P)\right) \\ &\leq \frac{\mathsf{E}[P_{far}]}{\Delta P/\beta} + \Pr\left(P_{near} \geq \frac{1}{\beta}(P_0-\Delta P)\right) \end{aligned} \quad (20)$$

where we used the Markov Inequality to bound the first term in (20). The expectation in the first term is readily evaluated as:

$$\begin{aligned}\mathsf{E}[P_{far}] &\equiv \frac{\rho}{2\pi}\int_{\hat{r}=R_{th}}^{\infty}\int_{\phi_1,\phi_2=-\pi}^{\pi} P_0 g(\phi_1)g(\phi_2)\frac{R_0^2}{r^2}e^{-\alpha(r-R_0)} \; r dr\ d\phi_1\ d\phi_2 \\ &= \frac{(\Delta\phi)^2}{2\pi}P_0(\rho R_0^2)e^{\alpha R_0}\int_{r=R_{th}}^{\infty}\frac{e^{-\alpha r}}{r}dr \\ &\lessapprox \frac{(\Delta\phi)^2}{2\pi}\frac{P_0(\rho R_0^2)}{\alpha R_{th}}e^{\alpha(R_0-R_{th})} \end{aligned} \quad (21)$$

D. A pseudo-wired abstraction

Figs. 4 and 5 show the collision probabilities for ideal "flat-top" arrays and for linear arrays with $\rho R_0^2 = 1$ and $\alpha = 10$ dB/km and beamwidth=10° and different values of the SINR threshold β. The probabilities were computed analytically from (18) and also from (20) where the second term in (20) was evaluated by the use of Monte-Carlo simulations and the first term from (21) with $R_{th} = 40R_0$ and $\Delta P = P_0 - 30$ dB.

We observe that when the desired SINR β increases beyond about 15 dB, the probability of collision approaches 10%. However, for the parameters corresponding to the reference link budget described in Section II, the collision probabilities are very small (less than 4%). Furthermore, in this highly directional regime, the probability of collision under the physical model does not appreciably differ from the protocol

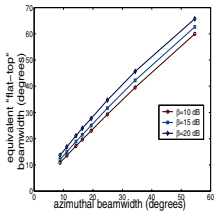

Fig. 3. Flat-top beamwidth.

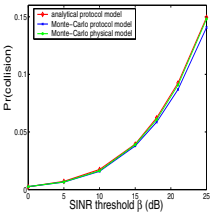

Fig. 4. Flat-top antenna.

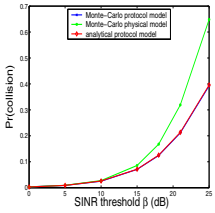

Fig. 5. Linear array.

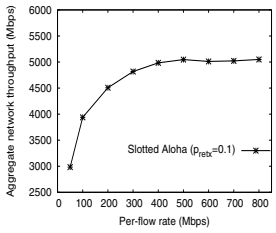

Fig. 6. Aggregate network throughput versus per-flow rate.

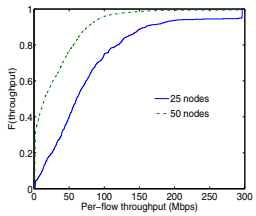

Fig. 7. Per-flow throughput empirical CDF versus node density.

model. This indicates that we may not need to worry about far-away interferers or the details of antenna beam patterns (using the notion of the equivalent flat-top beamwidth). We conclude that the MAC designer can use the following **pseudo-wired abstraction:** as a starting point: (1) *Half-duplex constraint.* Each node can either transmit or receive at any given time but not both. (2) *No interference.* Transmissions between two distinct pair of nodes are unlikely to interfere with each other, and can be largely ignored in MAC design.

IV. MAC Simulations

To verify the pseudowired abstraction, we simulate a naive slotted Aloha protocol (prior studies on slotted Aloha with directional communication include [8]–[10], but our goal is to examine the relative effects of interference and deafness on performance). We note that far better performance can be obtained using more sophisticated MAC designs; this is a topic of ongoing research to be reported in later publications.

Simulation set-up: We consider random network topologies with 25 or 50 nodes spread over a 500m x 500m flat terrain. Every node initiates one constant bit rate (CBR) flow to each of its neighbors. Whenever a node has a new packet to transmit, it beamforms towards the direction of the intended receiver and transmits the packet in the next slot. If the node does not receive an ACK, it attempts to retransmit the packet with a probability p_{retx} over the next slots. A node returns to the unbacklogged state after every successful packet transmission. We consider a sectorized antenna design with each sector covered by an array of high-gain horn elements (e.g., a linear array of four horn elements of directivity 18dBi each achieves the total directivity of 24dBi, with the horizontal sector-span of 20 degrees.) We use the QualNet Network Simulator [11], modifying the QualNet PHY and Antenna modules to model propagation in the mm-wave band and our link budget design.

Fig. 6 shows (for 25 nodes) the aggregate network throughput versus network load, with $p_{retx} = 0.1$. The throughput is significantly higher than with omnidirectional Aloha. Fig. 7 plots the empirical cumulative distribution function of the per-flow throughput for slotted Aloha for an input per-flow rate of 300Mbps for 25 and 50 node random topologies over a fixed terrain. Clearly, naive Aloha does not achieve anywhere near fair resource allocation among flows. The average throughput per flow decreases with node density: having more neighbors makes transmit-receive coordination more difficult, and increases interference. However, packet losses due to failed coordination are an order of magnitude higher than those due to interference: the fractions of failed receptions relative to the total received packets because of interference and failed coordination are 2.2% and 35.7%, respectively, for 25 nodes, and 5.6% and 47.2% for 50 nodes.

V. Conclusions

We have pointed out how the unique physical layer characteristics of mm wave links impact MAC design. Our interference analysis framework enables a quantitative evaluation of when we can model highly directive links as pseudo-wired. For the directivities typical of mm wave nodes with compact form factors, the pseudo-wired model is indeed appropriate, which motivates a radically different approach to MAC design. Rather than focusing on interference management as in conventional MAC design, we must now devise scheduling mechanisms that address deafness.

References

[1] R. R. Choudhury, X. Yang, R. Ramanathan, and N. H. Vaidya, "On designing mac protocols for wireless networks using directional antennas," *IEEE Trans. Mob. Comput.*, vol. 5, no. 5, pp. 477–491, 2006.

[2] R. Ramanathan, J. Redi, C. Santivanez, D. Wiggins, and S. Polit, "Ad hoc networking with directional antennas: a complete system solution," *IEEE J. Sel. Areas Commun.*, vol. 23, no. 3, pp. 496–506, March 2005.

[3] T. Korakis, G. Jakllari, and L. Tassiulas, "Cdr-mac: A protocol for full exploitation of directional antennas in ad hoc wireless networks," *IEEE Trans. Mob. Comput.*, vol. 7, no. 2, pp. 145–155, Feb. 2008.

[4] C. Bettstetter, C. Hartmann, and C. Moser, "How does randomized beamforming improve the connectivity of ad hoc networks?" *IEEE ICC'05*, vol. 5, pp. 3380–3385, May 2005.

[5] H. Koskinen, "Analytical study of connectivity in wireless multihop networks utilizing beamforming," in *Proc. ACM MSWiM '06*, 2006, pp. 212–218.

[6] P. Gupta and P. R. Kumar, "The capacity of wireless networks," *IEEE Trans. Inform. Theory*, vol. 46, no. 2, pp. 388–404, 2000.

[7] R. Mudumbai and U. Madhow, "Information theoretic bounds for sensor network localization," in *Proc. IEEE ISIT'08*, July 2008, pp. 1602–1606.

[8] J. Zander, "Slotted aloha multihop packet radio networks with directional antennas," *Electronics Letters*, vol. 26, no. 25, pp. 2098–2100, Dec. 1990.

[9] J. Ward and J. Compton, R.T., "Improving the performance of a slotted aloha packet radio network with an adaptive array," *Communications, IEEE Transactions on*, vol. 40, no. 2, pp. 292–300, Feb 1992.

[10] H. Singh and S. Singh, "Smart-aloha for multi-hop wireless networks," *Mob. Netw. Appl.*, vol. 10, no. 5, pp. 651–662, 2005.

[11] (2007) Qualnet Network Simulator, version 4.0. [Online]. Available: http://www.scalable-networks.com